Article

Generalized Full Order Observer Subject to Incremental Quadratic Constraint (IQC) for a Class of Fractional Order Chaotic Systems

Muhammad Marwan *[ID]**, Muhammad Zainul Abidin** *[ID]**, Humaira Kalsoom** [ID] **and Maoan Han**

College of Mathematics and Computer Science, Zhejiang Normal University, Jinhua 321004, China; humaira87@zju.edu.cn (H.K.); mahan@zjnu.edu.cn (M.H.)
* Correspondence: marwan78642@zjnu.edu.cn (M.M.); mzainulabidin@zjnu.edu.cn (M.Z.A.)

Abstract: In this paper, we used Lyapunov theory and Linear Matrix Inequalities (LMI) to design a generalized observer by adding more complexity in the output of the dynamic systems. Our designed observer is based on the optimization problem, minimizing error between trajectories of master and slave systems subject to the incremental quadratic constraint. Moreover, an algorithm is given in our paper used to demonstrate a method for obtaining desired observer and gain matrixes, whereas these gain matrixes are obtained with the aid of LMI and incremental multiplier matrix (IMM). Finally, discussion of two examples are an integral part of our study for the explanation of achieved analytical results using MATLAB and SCILAB.

Keywords: dynamic systems; fractional order chaotic systems; observer; synchronization; incremental quadratic constraint; linear matrix inequalities

1. Introduction

A system of differential equations of the form $\dot{\mathfrak{z}}_i = \Psi_i(\mathfrak{z}_i); i = 1, 2, \cdots, n$ is said to be a dynamic system, whereas a special property in which a dynamic system is sensitive to initial conditions and parameters involved in given system is known as a chaotic system. It was Lorenz in 1963, the pioneer of chaos, who found unpredictability for the first time in observing a climate-based system. Since then, infinitely many chaotic systems were derived. The variety of their applications can be found in several fields other than mathematics such as finance [1,2], medicine [3–5], biology [6,7] and environmental science [8]. However, apart from above applications, chaos can be found in engineering-based subjects as well. In 2017, Qi considered the brushless DC motor [9] and analyzed its chaotic dynamics by decomposing their torque terms into four parts using the energy casimir function. The chaotic dynamics and multi-pulse orbits in cantilevered pipes for conveying pulsating fluid with harmonic force are discussed with the aid of energy-phase method in [10]. A four rotor-based drone [11] is being considered by Bi et al. for detecting chaos using energy functions. In 2019, Yang and Qi [12] worked on plasma chaotic system using generalized competitive mode and mechanism analysis for the discussion of its various dynamic modes.

In 1823, Abel used a technique based on fractional calculus for the first time while investigating a physical problem and then Liouville followed the same work by introducing physical applications of fractional calculus into potential theory. Since then, this topic spread to other fields such as inequalities [13,14], optimization [15], nonlinear dynamics [16], cyber-security [17] and many more. Fractional calculus has a great influence on chaotic systems and its impact can be seen not only in detecting chaos, but also a variety of work can be found in bifurcation [18–20], synchronization [16,21] and stability [22,23]. Fractional derivatives in dynamic systems is one of the most interesting topics for researchers at present. In 2020, Rajeev et al. [24] focused on the convergence of series solution in the fractional generalized Korteweg–de Vries equation. The Adomian decomposition scheme

is used as a solver for fractional order delay differential equations [25] and several other recent works in fractional calculus linking with dynamic systems can be found in [26–28] and the references there in.

A control-based strategy in which at least two identical or non-identical dynamic systems overlap their trajectories is known as synchronization. In other words, synchronization occurs when one or more drive systems start following a single master system. Several computer-based applications of synchronization can be found in the literature such as [29–31] and the references therein. Observers can be found as a best example of synchronization for engineering-based work and a system is said to be observable if $rank(A, B)$ is full ranked. In 2011, Açıkmeşe et al. [32] used implicit relationship with quadratic inequality constraint for chaotic system. Then, Lipshitz [33,34] and monotonic [35] inequalities satisfying IQC were used and in-response special matrixes were created. After that, Zhou et al. [36] combined IQC with the bounds of system as faces of octahedron and designed Incremental Multiplier Matrix (IMM). In 2020, Sabir et al. worked on an observer with single linear and nonlinear outputs for quadrotor chaotic system [37]. Recently in 2022, Liu et al. worked on observers for fractional order chaotic systems using functional impulsive response [38].

The above cited work and our knowledge of the literature reveals that a class of observers, satisfying incremental quadratic constraints, was confined to less non-linearity in output and integer ordered dynamic systems. This idea encouraged us to fill the gap in the literature by providing a scheme, which can help in the synchronization of master and slave system with more complexity in output for fractional as well as integer order dynamic systems. For this purpose, we have provided Theorem 1, Corollaries 1–3, Remark 2 and Algorithm 1 to attain generalized observer with n nonlinear outputs. The following five steps can be followed to make our methodology more feasible and user friendly:

1. Convert fractional/integer order dynamic systems into class (9).
2. Obtain the symmetric incremental multiplier matrix σ_m using the following inequality:

$$\begin{pmatrix} \sigma_{m11} + \sigma_{m12} \; \theta_i + \theta_i^T \sigma_{m12}^T & \theta_i^T \sigma_{m22} \\ \sigma_{m22} \, \theta_i & -\sigma_{m22} \end{pmatrix} > 0; \quad i = 1, 2, \cdots, 6 \qquad (1)$$

   for nonlinear function; $\mathfrak{f}(r)$ with faces of the octahedron; $\sum_{i=1}^{n} \mathfrak{z}_i \, \theta_i = \frac{\partial \mathfrak{f}}{\partial r}$.
3. Check the bound of dynamic system. If the system is bounded, then go to the next step. Otherwise, the method does not work here.
4. Use matrix; σ_m into inequality (27) to compute gain matrixes; $\mathcal{T}_q, \mathcal{T}_1, \mathcal{T}_{2j}; j = 1, 2, \cdots, n$ and symmetric matrix $\wp$.
5. Calculate generalized observer (10) by substituting matrixes obtained in step 4.

This paper follows the following pattern: Section 2 consists of basic results including definitions, Lemmas and remarks for the better understanding of rest of the work. In Section 3, we stated and proved Theorem 1 for generalized observer satisfying IQC with n nonlinear outputs. This section also contains an algorithm, which plays a vital role in obtaining the gain matrixes and procedure for achieving result of our designed observer. Numerical simulations for gain matrixes with suitable dimension and phase portraits for fractional order Lorenz and gyrostat chaotic systems were illustrated in Section 4. A comparison of our designed observer with other techniques is available in Section 5, while Section 6 contains the concluding remarks.

2. Prerequisite

Some basic definitions, theorems and lemmas are given in this section which can be helpful in understanding rest of the work. For convenience, a symmetric matrix $\mathcal{N} = \mathcal{N}^T$ can be rewritten as:

$$\mathcal{N} = \begin{pmatrix} \mathcal{N}_{11} & \star & \text{ⓢ} \\ \mathcal{N}_{12}^T & \mathcal{N}_{22} & \text{⊛} \\ \mathcal{N}_{13}^T & \mathcal{N}_{23}^T & \mathcal{N}_{33} \end{pmatrix} = \begin{pmatrix} \mathcal{N}_{11} & \mathcal{N}_{12} & \mathcal{N}_{13} \\ \mathcal{N}_{12}^T & \mathcal{N}_{22} & \mathcal{N}_{23} \\ \mathcal{N}_{13}^T & \mathcal{N}_{23}^T & \mathcal{N}_{33} \end{pmatrix} \tag{2}$$

in the mentioned form throughout our study.

Definition 1 ([32]). *A symmetric matrix:*

$$\sigma_m = \begin{pmatrix} \sigma_{m11} & \sigma_{m12} \\ \sigma_{m12}^T & \sigma_{m22} \end{pmatrix} \tag{3}$$

is said to be incremental multiplier matrix for nonlinear function $\mathfrak{f}(r)$, if the following condition is satisfied:

$$\begin{pmatrix} \Delta\mathfrak{z} \\ \Delta\mathfrak{f} \end{pmatrix}^T \sigma_m \begin{pmatrix} \Delta\mathfrak{z} \\ \Delta\mathfrak{f} \end{pmatrix} \geq 0, \tag{4}$$

where $\Delta\mathfrak{z} = \mathfrak{z} - \check{\mathfrak{z}}$ and $\Delta\mathfrak{f} = \mathfrak{f}(r) - \mathfrak{f}(\check{r})$, while condition given in inequality (4) is famous as Incremental Quadratic Constraint (IQC).

Several researchers worked on various types of inequalities satisfying incremental quadratic constraint. Here, Table 1 indicates the obtained increment matrix multiplier for special conditions on inequalities.

Table 1. Results of inequalities leading to special matrixes satisfying IQC.

Rule	Inequality	Condition	Matrix
Açıkmeşe et al. [32]	Incremental quadratic	Implicit relationship	$--$
Zhang et al. [33]	one-sided Lipschitz	$\Delta\Phi^T\Delta\mathfrak{z} \leq \rho\Delta\mathfrak{z}^T\Delta\mathfrak{z}$	$\beta\begin{pmatrix} \rho I & -\frac{1}{2}I \\ -\frac{1}{2}I & 0 \end{pmatrix}$
Zhou et al. [34]	Lipchitz	$\|\Delta\Phi\| \leq \gamma\|\Delta\mathfrak{z}\|$	$\beta\begin{pmatrix} \gamma^2 I & 0 \\ 0 & -I \end{pmatrix}$
Gupta et al. [35]	Generalized monotone	$\Delta\mathfrak{z}^T\Delta\Phi + \Delta\Phi^T\Delta\mathfrak{z} \geq \mu\Delta\mathfrak{z}^T\Delta\mathfrak{z}$	$\beta\begin{pmatrix} -\mu I & I \\ I & 0 \end{pmatrix}$
Zhao et al. [34]	non decreasing	$\Delta\mathfrak{z}^T\Delta\Phi \geq 0$	$\beta\begin{pmatrix} 0 & I \\ I & 0 \end{pmatrix}$

Finally, the following standard Lemmas will be useful in the proofs given in Section 3.

Lemma 1 ([39]). *Let $\mathfrak{R} = \begin{pmatrix} \mathfrak{R}_{11} & \mathfrak{R}_{12} \\ \mathfrak{R}_{12}^T & \mathfrak{R}_{22} \end{pmatrix}$ be a symmetric matrix. Then the following properties are equivalent:*

a. $\mathfrak{R} < 0,$
b. $\mathfrak{R}_{11} < 0, \mathfrak{R}_{22} - \mathfrak{R}_{12}^T\mathfrak{R}_{11}^{-1}\mathfrak{R}_{12} < 0,$
c. $\mathfrak{R}_{22} < 0, \mathfrak{R}_{11} - \mathfrak{R}_{12}\mathfrak{R}_{22}^{-1}\mathfrak{R}_{12}^T < 0.$

Lemma 2 ([40]). *Let us consider $\mathcal{W} = \mathfrak{z}^T\wp\mathfrak{z}$ with a symmetric matrix; $\wp$. Then, it holds*

$$\lambda_{min}(\wp)\|\mathfrak{z}\|^2 \leq \mathcal{W} \leq \lambda_{max}(\wp)\|\mathfrak{z}\|^2, \tag{5}$$

where $\lambda_{min}(\wp), \lambda_{max}(\wp)$ are the minimum and maximum eigenvalues of $\wp$.

Lemma 3 ([41]). *Suppose $\nabla(\cdot)$ be an uncertain function satisfying inequality (6). Then, there exists a non-negative function γ, such that:*

$$(a - b)(\Psi(a) - \Psi(b) + \nabla(a)\varphi_m) \geq -\gamma|\varphi_m|, \tag{6}$$

where a, b, φ_m are in real number set.

Here in this work, we tried to design an observer for fractional order chaotic systems. Therefore, this portion concerns with some basics about fractional derivatives.

Definition 2. *Let us consider a function $g(w)$, then its fractional order integration can be defined as:*

$$I_{w_0}^{\beta} g(w) = \int_{w_0}^{w} \frac{w - \tau}{\Gamma(\beta)} g(\tau) d\tau, \tag{7}$$

where β is any non$-$integer number.

Remark 1. *If $w_0=0$ is used into Equation (7), then one can write $I_0^{\beta} = g(w) \circledast \phi(w)$, where $\circledast$ is convolution operator and*

$$\phi(w) = \begin{cases} \frac{w^{\beta-1}}{\Gamma(\beta)} & ; \quad w > 0 \\ 0 & ; \quad w \leq 0. \end{cases}$$

The work of Caputo in 1967 on derivative, famous as Caputo's Derivative (*CD*), was the generalized form of derivatives in fractional calculus and played important role in Fractional Order Dynamic Systems (FODS). Several researchers have been working on modification of *CD* in recent decades. However, the *CD*, which researchers are using in the field of nonlinear analysis for fractional order systems can be found in [42].

Definition 3. *Fractional order derivative of a function $g(w)$ is defined as:*

$$D_{w_0}^{\beta} g(w) = \frac{d}{dw} \int_{w_0}^{w} \frac{w - \tau}{\Gamma(1 - \beta)} g(\tau) d\tau. \tag{8}$$

We used a fractional derivative for achieving a solution for chaotic systems.

3. Generalized Observer for FOCS

In this section, a theorem is proved to design generalized observer for a class of fractional order chaotic systems. The proposed observer can cover a wide range of chaotic systems such as [43–45]. Throughout this section, we consider $\mathfrak{F}_{os}$ as a class of fractional ordered chaotic systems of the form:

$$\mathfrak{F}_{os} : \begin{cases} D^{\beta}\mathfrak{z} = \mathcal{A}\mathfrak{z} + \mathcal{B}\mathfrak{f}(r) + \varpi, \\ \mathfrak{y}_1 = \mathcal{C}\mathfrak{z}, \\ \mathfrak{y}_{2j} = \mathcal{D}_j[\Psi_j + \nabla_j(\nu)\varphi_{m_j}] \text{ for } j = 1, 2, \cdots, n, \end{cases} \tag{9}$$

where $\mathcal{A} \in \mathbb{R}^{k_1 \times k_1}, \mathcal{B} \in \mathbb{R}^{k_2 \times r}, \mathcal{C} \in \mathbb{R}^{k_{1a} \times k_2}, \mathcal{D}_j$ are scalar numbers and solution of system (9) belongs to euclidean space of k_1 tuples. Moreover, $\mathfrak{y}_1$ and $\mathfrak{y}_{2j}; j = 1, 2, \cdots, n$ are linear and nonlinear outputs of master system (9), whereas $r = \mathcal{G}\mathfrak{z}, \mathcal{G} \in \mathbb{R}^{k_q \times k_2}$ and $\nu = M\mathfrak{z}$ such that M is any real numbered row matrix of order $1 \times k_1$. A generalized observer for class (9) is:

$$D^{\beta}\check{\mathfrak{z}} = \mathcal{A}\check{\mathfrak{z}} + \mathcal{B}\mathfrak{f}(\check{r}) + \mathcal{T}_1(\mathfrak{y}_1 - \mathcal{C}\check{\mathfrak{z}}) + \sum_{j=1}^{n} \mathcal{T}_{2j}[\mathfrak{y}_{2j} - \mathcal{D}_j\Psi_j(\check{\nu})], \tag{10}$$

where $\check{\mathfrak{z}}$ is estimated state variable, while $\check{r} = \mathcal{G}\check{\mathfrak{z}} + \mathcal{T}_r(\mathfrak{y}_1 - \mathcal{C}\check{\mathfrak{z}})$ and $\check{v} = M\check{\mathfrak{z}}$ are estimations of r and v, respectively. The matrixes; $\mathcal{T}_r, \mathcal{T}_1, \mathcal{T}_{2j}, j = 1, 2, \ldots, n$ including in Equation (10) are real valued gain matrixes.

Theorem 1. *Suppose a system belongs to class* (9) *satisfying IQC, the matrix inequality:*

$$\begin{bmatrix} \wp(\mathcal{A} - \mathcal{T}_1\mathcal{C}) + (\mathcal{A} - \mathcal{T}_1\mathcal{C})^T\wp + (\mathcal{G} - \mathcal{T}_r\mathcal{C})^T\sigma_{m11}(\mathcal{G} - \mathcal{T}_r\mathcal{C}) + 2\alpha\wp & \star \\ \mathcal{B}^T\wp + \sigma_{m12}^T(\mathcal{G} - \mathcal{T}_r\mathcal{C})^T & \sigma_{m22} \end{bmatrix} \leq 0 \quad (11)$$

and the equality:

$$\wp \sum_{j=1}^{n} \mathcal{T}_{2j}\mathcal{D}_j - \gamma_j M_j^T = 0 \quad (12)$$

constraints hold with known increment multiplier matrix. Then, system (10) *is generalized observer for a class of fractional order chaotic systems* (9)*. Moreover, the error terms $\mathfrak{E}(t)$ are bounded and convergent for all $t \geq 0$.*

Proof. Control and synchronization-based strategies work on the concept of error dynamic system. Therefore, in our case error is the difference between $\mathfrak{z} \in \mathfrak{F}_{os}$ and estimated variable $\check{\mathfrak{z}}$:

$$\mathfrak{E}(t) = \mathfrak{z}(t) - \check{\mathfrak{z}}(t). \quad (13)$$

The fractional order derivative of Equation (13) is:

$$D^\beta \mathfrak{E}(t) = D^\beta \mathfrak{z}(t) - D^\beta \check{\mathfrak{z}}(t). \quad (14)$$

Putting Equations (9) and (10) into Equation (14) yields:

$$D^\beta \mathfrak{E}(t) = (\mathcal{A} - \mathcal{T}_1\mathcal{C})\mathfrak{E} + \mathcal{B}\Delta\mathfrak{f} - \sum_{j=1}^{n}\left(\mathcal{T}_{2j}\mathcal{D}_j[\Delta\Psi_j + \nabla_j(\check{v})\varphi_{m_j}]\right), \quad (15)$$

where $\Delta\mathfrak{f} = \mathfrak{f}(r) - \mathfrak{f}(\check{r})$ and $\Delta\Psi = \Psi(v) - \Psi(\check{v})$. Moreover, the difference between r and $\check{r}$ gives us:

$$\Delta r = (\mathcal{G} - \mathcal{T}_r\mathcal{C})\mathfrak{E}. \quad (16)$$

Now, using Equations (15) and (16) in combination with incremental multiplier matrix for $\mathfrak{E}$ and $\Delta\mathfrak{f}$ yields:

$$\begin{bmatrix} \mathfrak{E} \\ \Delta\mathfrak{f} \end{bmatrix}^T Y^T \sigma_m Y \begin{bmatrix} \mathfrak{E} \\ \Delta\mathfrak{f} \end{bmatrix} \geq 0, \quad (17)$$

where

$$Y = \begin{bmatrix} (\mathcal{G} - \mathcal{T}_r\mathcal{C}) & 0 \\ 0 & I \end{bmatrix}. \quad (18)$$

We select a quadratic Lyapunov function in terms of errors:

$$\mathcal{W}(\mathfrak{E}) = \mathfrak{E}^T\wp\mathfrak{E}. \quad (19)$$

Differentiating Equation (19) along its state trajectories:

$$
\begin{aligned}
D^{\beta}\mathcal{W}(t) \;=\;& \mathfrak{E}^{T}\Big[\wp(\mathcal{A}-\mathcal{T}_1\mathcal{C})+(\mathcal{A}-\mathcal{T}_1\mathcal{C})^{T}\wp\Big]\mathfrak{E}+\mathfrak{E}^{T}\wp\mathcal{B}\Delta\mathfrak{f}\\
&+\Delta\mathfrak{f}^{T}\mathcal{B}^{T}\wp\mathfrak{E}-2\sum_{j=1}^{n}\Big(\mathfrak{E}^{T}\wp\mathcal{T}_{2j}\mathcal{D}_{j}[\Delta\Psi_{j}+\nabla_{j}(\check{v})\varphi_{m_{j}}]\Big).
\end{aligned}
\tag{20}
$$

Rewriting Equation (20) into matrix form after shifting $2\sum_{j=1}^{n}\Big(\mathfrak{E}^{T}\wp\mathcal{T}_{2j}\mathcal{D}_{j}[\Delta\mathfrak{f}+\nabla_{j}(\check{v})\varphi_{m_{j}}]\Big)$ to the other side gives:

$$
\begin{aligned}
D^{\beta}\mathcal{W}(t) \;+\;& 2\sum_{j=1}^{n}\Big(\mathfrak{E}^{T}\wp\mathcal{T}_{2j}\mathcal{D}_{j}[\Delta\Psi_{j}+\nabla_{j}(\check{v})\varphi_{m_{j}}]\Big)\\
\;=\;& \begin{bmatrix} \wp(\mathcal{A}-\mathcal{T}_1\mathcal{C})+(\mathcal{A}-\mathcal{T}_1\mathcal{C})^{T}\wp-2\alpha\wp & \star \\ \mathcal{B}^{T}\wp & 0 \end{bmatrix}.
\end{aligned}
\tag{21}
$$

Finally, we obtain our desired result (1) by multiplying $[\mathfrak{E}^{T}\ \Delta\mathfrak{f}^{T}]^{T}$ from both ends with the right side of Equation (21) and then adding with the inequality (17). For bounded convergence of error term, we obtain the following inequality using Equations (20) and (21):

$$
D^{\beta}\mathcal{W}(t)+2\sum_{j=1}^{n}\Big(\mathfrak{E}^{T}\wp\mathcal{T}_{2j}\mathcal{D}_{j}[\Delta\Psi_{j}+\nabla_{j}(\check{v})\varphi_{m_{j}}]\Big)+2\alpha\mathcal{W}\leq 0.
\tag{22}
$$

In view of Lemma 3, inequality (22) can be rewritten as:

$$
\begin{aligned}
D^{\beta}\mathcal{W}(t) \;\leq\;& -2\left(\alpha\mathcal{W}+\sum_{j=1}^{n}\wp\mathcal{T}_{2j}\mathcal{D}_{j}\Big([\Delta\Psi_{j}+\nabla_{j}(\check{v})\varphi_{m_{j}}]\Big)\right)\\
\;\leq\;& -2\left(\alpha\mathcal{W}+\sum_{j=1}^{n}\gamma_{j}(v-\check{v})\Big([\Psi_{j}(v)-\Psi_{j}(\check{v})+\nabla_{j}(\check{v})\varphi_{m_{j}}]\Big)\right)\\
\;\leq\;& -2\alpha\mathcal{W}+2\sum_{j=1}^{n}\eta_{j}|\varphi_{m_{j}}|,
\end{aligned}
\tag{23}
$$

where $\wp\mathcal{T}_{2j}\mathcal{D}_{j}=\gamma_{j}\Delta v$. Solving inequality (23) for $\mathcal{W}$ gives:

$$
\mathcal{W}(t)\leq \mathcal{W}(0)\exp(-2\alpha t)+\sum_{j=1}^{n}\left(\frac{\gamma_{j}\eta_{j}|\varphi_{m_{j}}|}{\alpha}\right).
\tag{24}
$$

From Equation (19), one can observe that $\mathcal{W}$ is the combination of error term $\mathfrak{E}$ and symmetric matrix $\wp$. Therefore, in view of Lemma 2, inequality (24) can be rewritten as:

$$
\begin{aligned}
\lambda_{\min}(\wp)||\mathfrak{E}(t)||^{2} \;\leq\;& \mathcal{W}(t)\leq \lambda_{\max}(\wp)||\mathfrak{E}(t)||^{2}\\
\;\leq\;& \lambda_{\max}(\wp)||\mathfrak{E}(0)||^{2}\exp(-2\alpha t)+\sum_{j=1}^{n}\left(\frac{\gamma_{j}\eta_{j}|\varphi_{m_{j}}|}{\alpha}\right).
\end{aligned}
\tag{25}
$$

Hence,

$$
\mathfrak{E}(t)\leq \mathfrak{E}_{0}\exp(-2\alpha t)+\sqrt{\sum_{j=1}^{n}\left(\frac{\gamma_{j}\eta_{j}|\varphi_{m_{j}}|}{\alpha\lambda_{\min}\wp}\right)},
\tag{26}
$$

where $\mathfrak{E}_{0}$ is the ratio between max and min eigenvalues of a symmetric matrix $\wp$. This completes our required proof and shows that the observer given in Equation (10) synchronizes

to class of fractional order chaotic systems (9) after some time 't' with the convergence of error term. □

3.1. Lmis and Algorithm for Gain Matrices

We designed an algorithm in this section to find gain matrixes $\mathcal{T}_r, \mathcal{T}_1, \mathcal{T}_{2j}; j = 1, 2, \cdots, n$ and a symmetric matrix $\wp$, which are helpful in the calculation of an observer system (10). For linear matrix inequalities, we use Shurs Lemma 1 on inequality (11) to obtain:

$$
\begin{bmatrix}
\Omega_\wp & \star & \circledS \\
\mathcal{B}^T \wp + \sigma_{m12}^T (\mathcal{G} - \mathcal{T}_r \mathcal{C})^T & \sigma_{m22} & 0 \\
(\mathcal{G} - \mathcal{T}_r \mathcal{C})_{11}^{\sigma_m} & 0 & -\sigma_{m11}
\end{bmatrix} \leq 0,
\tag{27}
$$

where $\Omega_\wp = 2\alpha\wp + \wp\mathcal{A} + \mathcal{A}^T \wp - (\mathcal{Q}\mathcal{C} + \mathcal{C}^T \mathcal{Q}^T)$ such that $\mathcal{Q} = \wp\mathcal{T}_1$. Inequality given in (27) can also be useful in achieving the feasibility condition of obtained solution.

Corollary 1. *Let us suppose $j = 1$ into system (10) with $\beta = 1$ then, we obtain the observer given in [36].*

Corollary 2. *Suppose $\beta = [\beta_1, \beta_2, \beta_3]$ is considered 1 in system (9). Then, observer (10) is valid for integer ordered chaotic systems.*

Corollary 3. *Introducing $\mathcal{D}_j = 0$ into system (10), then one can achieve results of [35,41].*

4. Numerical Simulations

In this section, we used fractional order Lorenz and Gyrostat chaotic systems as examples for using Algorithm 1 in the finding of gain matrixes and trajectories of generalized full order observer.

Algorithm 1 Generalized full order observer for a class of fractional order chaotic systems

---

1　We transform any fractional order chaotic system into the form (9).
2　The algorithm given in [36] is used to achieve the matrix σ_m for $\mathfrak{f}(r)$.
3　Then, we use σ_m into inequality given in (27) to compute all unknown symmetric and gain matrixes.
4　Finally, we compute generalized full order observer (10) with n nonlinear outputs for a class of systems (9).

4.1. Fractional Order Lorenz Chaotic System

Our first example is fractional order Lorenz system [46]:

$$
\begin{cases}
D_{\beta_1}\mathfrak{z}1 = \sigma(\mathfrak{z}2 - \mathfrak{z}1), \\
D_{\beta_2}\mathfrak{z}2 = \rho\mathfrak{z}1 - \mathfrak{z}2 - \mathfrak{z}1\mathfrak{z}3, \\
D_{\beta_3}\mathfrak{z}3 = \mathfrak{z}1\mathfrak{z}2 - b\mathfrak{z}3,
\end{cases}
\begin{cases}
\mathfrak{y}_{1a} = \mathfrak{z}1 + \mathfrak{z}2, \\
\mathfrak{y}_{2a} = \mathfrak{z}3, \\
\mathfrak{y}_{3a} = \mathfrak{z}3,
\end{cases}
\begin{cases}
\mathfrak{y}_{21} = \mathcal{D}_1[(M_1\mathfrak{z})^4 + v_1], \\
\mathfrak{y}_{22} = \mathcal{D}_1[(M_2\mathfrak{z})^2 + v_2], \\
\mathfrak{y}_{23} = \mathcal{D}_1[(M_3\mathfrak{z})^3 + v_3],
\end{cases}
\tag{28}
$$

where $M_1 = [5, -3, 1]$, $M_2 = [2, 0, -7]$, $M_3 = [1, 2, 0]$, $\mathcal{D}_i = 10^{-5}$, while $\mathfrak{y}_1 = [\mathfrak{y}_{1a}, \mathfrak{y}_{1b}, \mathfrak{y}_{1c}]^T$ is the linear output. System (28) can be transformed into class (9) with:

$$
\mathcal{A} = \begin{bmatrix} -\sigma & \sigma & 0 \\ \rho & -1 & 0 \\ 0 & 0 & -b \end{bmatrix}, \quad
\mathcal{B} = \begin{bmatrix} 0 & 0 \\ -1 & 0 \\ 0 & 1 \end{bmatrix}, \quad
\mathfrak{f}(r) = \begin{bmatrix} r_1 r_3 \\ r_1 r_2 \end{bmatrix}
\tag{29}
$$

and ϖ is zero column matrix of order 3. The faces of octahedron using $\frac{\partial \mathfrak{f}}{\partial r}$ and incremental multiplier matrix σ_m for system (28) can be found in [36]. The above information is useful in achieving the following gain matrixes:

$$\mathcal{T}_q = \begin{bmatrix} 1.0044 & 0.138 & 0.773 \\ 0.0004 & -4.6995 & -1.6966 \\ 0 & 0.6813 & 0.262 \end{bmatrix}, \ \mathcal{T}_1 = \begin{bmatrix} 40.5 & 0.0002 & -30.4942 \\ 0.0026 & 1396.6371 & 6973.1994 \\ 0.0042 & 4713.7746 & -306.98629 \end{bmatrix},$$

$$\mathcal{T}_{21} = \begin{bmatrix} 2703.57 \\ -8004949.35 \\ 3525593.882 \end{bmatrix}, \ \mathcal{T}_{22} = \begin{bmatrix} 1081.05 \\ 810376.06 \\ -2.224 \end{bmatrix}, \ \mathcal{T}_{23} = \begin{bmatrix} 540.79 \\ 5259454.389 \\ -231535.941 \end{bmatrix}. \tag{30}$$

Theorem 1 is proved for *n* nonlinear outputs, but for convenience, we are considering three nonlinear outputs.

In Figure 1, we can observe six trajectories moving with respect to time, in which the full dashed lines shows trajectories of fractional order chaotic system (28) and double dashed lines illustrates observer that is designed in Equation (10). It is further observed in the same figure that $\breve{\mathfrak{z}}$ overlap and follow path of $\mathfrak{z}$ as time advances and error dynamic system (15) approach to zero.
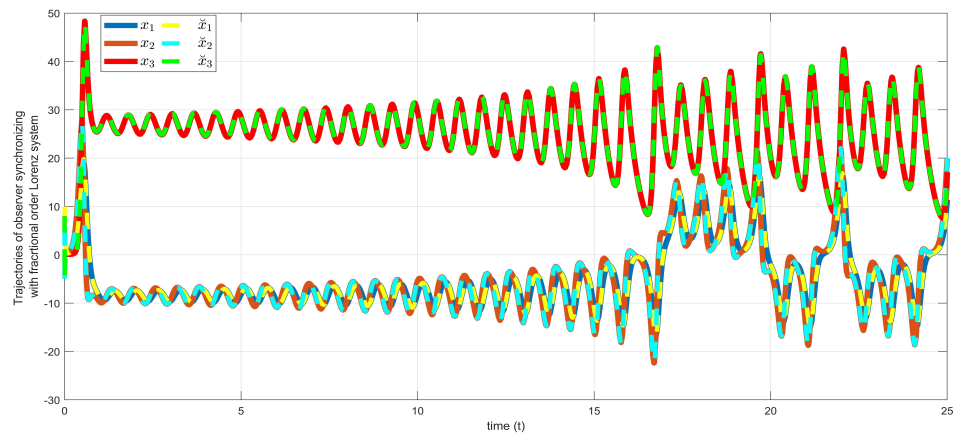

Figure 1. Trajectories of observer and fractional order Lorenz chaotic system.

Remark 2. *Let us consider* $\beta_1 = \beta_2 = \beta_3 = 1$ *with single nonlinear output* $\mathcal{T}_{21}$ *in Equation* (28), *then we can obtain results of Zhou et al.* [36].

4.2. Fractional Order Gyro Chaotic System

Our second example is fractional order Gyrostat system [47], which is not discussed anywhere in the field of control theory for observers. Therefore in this section, we will find its incremental multiplier matrix; *IMM* as well:

$$\begin{cases} I_a D_{\beta_1}\mathfrak{z}_1 = (I_b - I_c)\mathfrak{z}_2\mathfrak{z}_3 - h_c\mathfrak{z}_2 + h_b\mathfrak{z}_3 - \mu_a\mathfrak{z}_1 + L_a, \\ I_b D_{\beta_2}\mathfrak{z}_2 = (I_c - I_a)\mathfrak{z}_1\mathfrak{z}_3 + h_c\mathfrak{z}_1 + \mu_b\mathfrak{z}_2 + L_b, \\ I_c D_{\beta_3}\mathfrak{z}_3 = (I_a - I_b)\mathfrak{z}_1\mathfrak{z}_2 - h_b\mathfrak{z}_1 - \mu_c\mathfrak{z}_3 + L_c, \end{cases}$$

$$\begin{cases} \mathfrak{y}_{1a} = \mathfrak{z}_1 + 3\mathfrak{z}_2 - 2\mathfrak{z}_3, \\ \mathfrak{y}_{2a} = \mathfrak{z}_2 + 3\mathfrak{z}_3, \\ \mathfrak{y}_{3a} = 4\mathfrak{z}_1 + \mathfrak{z}_2, \end{cases} \begin{cases} \mathfrak{y}_{21} = \mathcal{D}_1[(M_1\mathfrak{z})^2 + v_1], \\ \mathfrak{y}_{22} = \mathcal{D}_2[(M_2\mathfrak{z})^5 + v_2], \\ \mathfrak{y}_{23} = \mathcal{D}_3[(M_3\mathfrak{z})^3 + v_3], \end{cases} \tag{31}$$

where $M_1 = [1, 3, 2]$, $M_2 = [5, 2, -2]$, $M_3 = [1, 2, 19]$, $\mathcal{D}_i = 10^{-5}$, while $\mathfrak{y}_1 = [\mathfrak{y}_{1a}, \mathfrak{y}_{1b}, \mathfrak{y}_{1c}]^T$ is linear output. System (31) can be transformed into class (9) with:

$$\mathcal{A} = \begin{bmatrix} -\frac{\mu_a}{I_a} & -\frac{h_c}{I_a} & \frac{h_b}{I_a} \\ \frac{h_c}{I_b} & \frac{\mu_b}{I_b} & 0 \\ -\frac{h_b}{I_c} & 0 & -\frac{\mu_c}{I_c} \end{bmatrix}, \ \mathfrak{f}(r) = \begin{bmatrix} r_2 r_3 \\ r_1 r_3 \\ r_1 r_2 \end{bmatrix}, \tag{32}$$

$\mathcal{B} = diag\left(\frac{I_b - I_c}{I_a}, \frac{I_c - I_a}{I_b}, \frac{I_a - I_b}{I_c}\right)$ and $\mathcal{O} = \left[\frac{L_a}{I_a}, \frac{L_b}{I_b}, \frac{L_c}{I_c}\right]^T$. System (31) is integer order for $\beta_1 = \beta_2 = \beta_3 = 1$ and is obviously chaotic [47]. However, for $\beta_1, \beta_2, \beta_3 = \beta \in [0.80, 0.99]$, system (31) is fractional order. Figure 2 shows $3D$ phase portrait of fractional order gyrostat chaotic system for different values of β. Physically, trajectories of gyrostat are momentum in their respective axis. Therefore, Figure 2 illustrates the unpredictable attitude of momentum in gyrostat with the advancement in time. These unpredictabilities occur due to negligible changes in the initial condition or bifurcation parameter.

(**a**) Single scrolled fractional order   (**b**) Multi scrolled fractional order
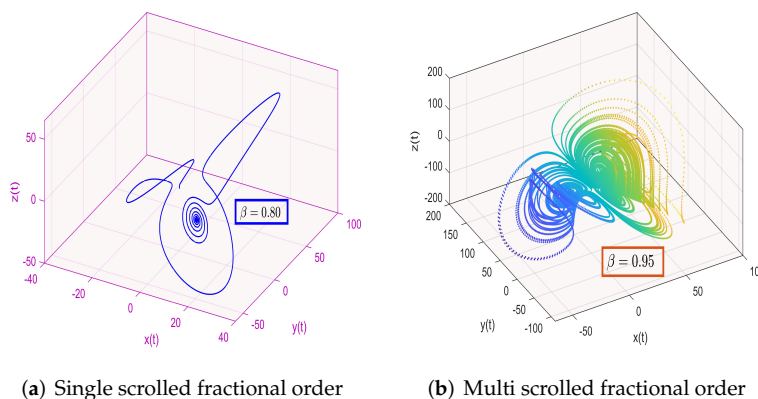
Figure 2. Three dimensional phase portraits of single to multi scrolled fractional order gyro chaotic system for $\beta \in [0.80, 0.99]$.

According to second step in Algorithm 1, we differentiate the nonlinear part $\mathfrak{f}(r)$ given in Equation (32) with respect to r for faces of the octahedron tangent to the edges of hyperboloid:

$$\Theta_1 = \rho \begin{pmatrix} 0 & 0 & 0 \\ 0 & 0 & 1 \\ 0 & 1 & 0 \end{pmatrix}, \quad \Theta_2 = \rho \begin{pmatrix} 0 & 0 & 1 \\ 0 & 0 & 0 \\ 1 & 0 & 0 \end{pmatrix}, \quad \Theta_3 = \rho \begin{pmatrix} 0 & 1 & 0 \\ 1 & 0 & 0 \\ 0 & 0 & 0 \end{pmatrix}, \tag{33}$$

and $\Theta_{4,5,6} = -\Theta_{1,2,3}$, where ρ is the hyperboloid bound [47] of gyrostat chaotic system:

$$\mu_a \left(\mathfrak{z}_1 - \frac{L_a}{2\mu_a}\right)^2 - \mu_b \left(\mathfrak{z}_2 - \frac{L_b}{2\mu_b}\right)^2 + \mu_c \left(\mathfrak{z}_3 - \frac{L_c}{2\mu_c}\right)^2 \leq 22.409. \tag{34}$$

The incremental multiplier matrix σ_m for system (31), with the aid of faces of octahedron (33), hyperboloid bound (34) and algorithm in [36], is:

$$\sigma_m = \begin{bmatrix} 53159.2564 & 0 & 0 & -13.6991 & 0 & 0 \\ 0 & 53159.2564 & 0 & 0 & -13.6991 & 0 \\ 0 & 0 & 53159.2564 & 0 & 0 & -13.6991 \\ -13.6991 & 0 & 0 & -61.315 & 0 & 0 \\ 0 & -13.6991 & 0 & 0 & -61.315 & 0 \\ 0 & 0 & -13.6991 & 0 & 0 & -61.315 \end{bmatrix}. \tag{35}$$

According to third step given in Section 1, our proposed observer work if given dynamic system is bounded. Therefore, it is observed in Figure 3 that system (31) is bounded by a hyperboloid (34) whose edges are tangent to an octahedron, whereas faces of octahedron are achieved using Equation (33). Gain matrixes for fractional order gyro chaotic system:

$$
\mathcal{T}_q = \begin{bmatrix} 0.7276 & 0 & -0.7276 \\ 0 & 0 & 1.544 \\ 0 & 0.4863 & 0 \end{bmatrix}, \; \mathcal{T}_1 = \begin{bmatrix} 454.3538 & -1.2307 & -455.3502 \\ 0 & 0 & 2062.4869 \\ 0 & 3521.76 & 0 \end{bmatrix},
$$

$$
\mathcal{T}_{21} = \begin{bmatrix} 0.9111 \\ 8.0152 \\ 9.4217 \end{bmatrix}, \; \mathcal{T}_{23} = \begin{bmatrix} 45555.59 \\ 53434.66 \\ -94216.53 \end{bmatrix}, \; \mathcal{T}_{24} = \begin{bmatrix} 9111.12 \\ 53434.66 \\ 895058.04 \end{bmatrix}. \tag{36}
$$

are obtained by following steps mentioned in Algorithm 1 using Equation (27).
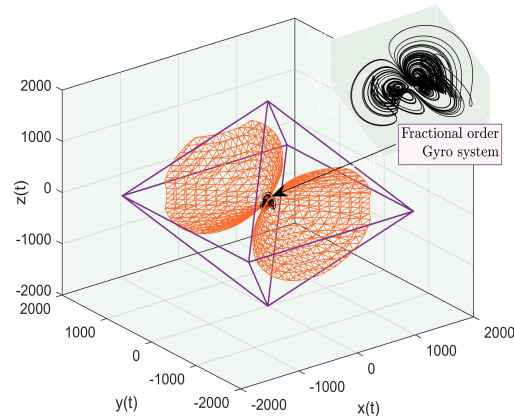
Figure 3. Bounded fractional order Gyro chaotic system inside octahedron.

Figure 4 illustrates synchronization of fractional gyro chaotic system and its observer. For the convenience of readers, we have zoom a part of Figure 4, where especially synchronization takes place. This shows that our designed observer works well in fractional order chaotic systems. There are many nonlinear terms included for bringing more complexity, but both examples show that the designed Algorithm 1 is generalized form for fractional as well as integer order chaotic systems.
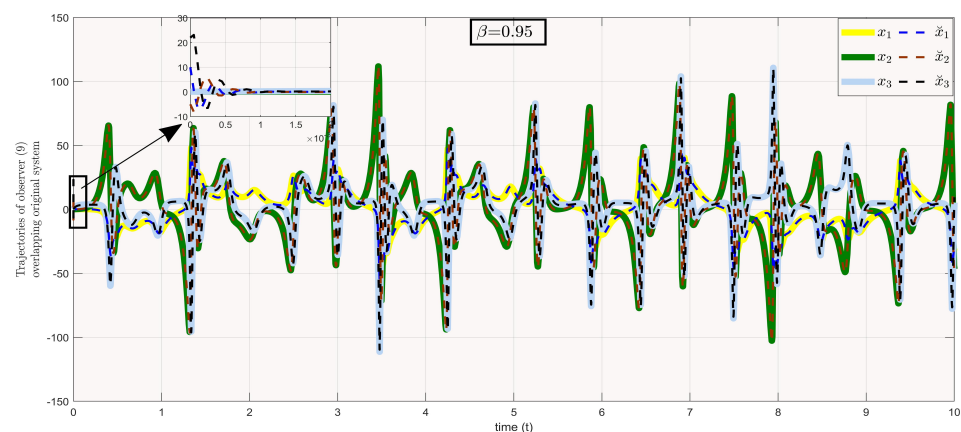
Figure 4. Trajectories of observer and fractional order Gyrostat chaotic system.

5. Comparison between Observers for Dynamic Systems

Since the usage of control inputs in synchronization, variety of techniques have been established. There are several applications of synchronization in engineering, but designing a suitable observer is the main focus of interest in present research. This paper shows design of a generalized full order observer for a class of dynamic systems, which can cover both fractional as well as integer order. comparison between different methods for the accuracy of our technique is presented in Table 2.

Table 2. Comparison between observers for dynamic systems.

Rule	IQC & σ_m	Order of System	Numbers of Nonlinear Outputs
Lan et al. [48]	No	Integer	1
Zulfiqar et al. [49]	No	Integer	1
Assaad et al. [50]	No	Fractional	1
Zhao et al. [51]	Yes	Integer	1
Moysis et al. [52]	No	Rectangular integer	1
Moysis et al. [53]	Yes	Rectangular integer	1
Zhao et al. [36]	Yes	Integer	1
Liu et al. [38]	Yes	Fractional	1
Our method	Yes	Integer/ Fractional	n

Mostly, observers subject to incremental quadratic constraints were limited to single nonlinear output, but our method is the most generalized form and can handle a lot of nonlinearity for fractional as well as integer order dynamic systems. Apart from generalization, our technique has a demerit; if the dynamic system is unbounded, then our technique does not work.

6. Conclusions

Based on the LMI and incremental quadratic constraints, this paper presents a generalized synchronization-based problem. In this paper, we showed that trajectories of two systems (integer and fractional order) can be synchronized with the help of observer composed of n nonlinear outputs. First, we defined a class, which consist of fractional as well as integer order dynamic systems. Then, an observer (10) is designed for our proposed class (9) in such a way that trajectories of slave system approaches to master system as time t tends to infinity. Theorem 1 was stated and proved for obtaining the bound of error term between systems (9) and (10), which helped in the convergence of estimated variables, while for numerical simulations an Algorithm 1 given in Section 3.1 can be followed. Moreover, Corollaries 1–3 and Remark 2 were provided to make it clear that our proposed observer was generalized and not confined to fractional order. To make it more clear and precise for readers, we discussed the given analytical results through two examples, in which the second example is explained in depth. Finally, a Table 2 was given in Section 5 for observing the accuracy of our proposed observer by comparison with other techniques.

Author Contributions: Conceptualization, M.M., M.Z.A. and H.K.; methodology, M.M., and H.K.; software, M.M.; validation, M.M., M.Z.A., H.K. and M.H.; formal analysis, M.M. and M.Z.A.; investigation, M.Z.A.; resources, H.K.; writing—original draft preparation, M.M., M.Z.A., H.K. and M.H.; writing—review and editing, M.M., M.Z.A., H.K. and M.H.; supervision, M.H.; project administration, M.M. and M.Z.A. All authors have read and agreed to the published version of the manuscript.

Conflicts of Interest: All authors declare no conflict of interest.

References

1. Cai, G.; Huang, J. A new finance chaotic attractor. *Int. J. Nonlin. Sci.* **2007**, *3*, 213–220.
2. Sundarapandian, V.; Aceng, S.; Sezgin, K.; Unal, C. A new finance chaotic system, its electronic circuit realization, passivity based synchronization and an application to voice encryption. *Nonlin. Eng.* **2019**, *8*, 193–205. [CrossRef]
3. Iqbal, J.; Ahmad, S.; Marwan, M.; Shaukat, M. Control and numerical analysis for cancer chaotic system. *Arch. Appl. Mech.* **2020**, *90*, 2597–2608. [CrossRef]
4. Uthamacumaran, A. A review of dynamical systems approaches for the detection of chaotic attractors in cancer networks. *Patterns* **2021**, *2*, 100226. [CrossRef] [PubMed]

5. Debbouche, N.; Ouannas, A.; Batiha, I.; Grassi, G. Chaotic dynamics in a novel COVID-19 pandemic model described by commensurate and incommensurate fractional-order derivatives. *Nonlin. Dyn.* **2021**, *2021*, 1–13. [CrossRef] [PubMed]

6. Behzad, G. On detecting chaos in a prey-predator model with prey's counter-attack on juvenile predators. *Chaos Solitons Fractals* **2021**, *150*, 111136. [CrossRef]

7. Balram, D.; Sajan; Ankit, K. Stability switching and chaos in a multiple delayed prey–predator model with fear effect and anti-predator behavior. *Math. Comp. Simul.* **2021**, *188*, 164–192. [CrossRef]

8. Cojocaru, V.P. Sensors based on chaotic systems for environmental monitoring. In *Improving Disaster Resilience and Mitigation—IT Means and Tools*; Springer: Dordrecht, The Netherlands, 2014; Volume 188, pp. 323–334. [CrossRef]

9. Guoyuan, Q. Energy cycle of brushless DC motor chaotic system. *Appl. Math. Model.* **2017**, *51*, 686–697. [CrossRef]

10. Zhang, Y.F.; Yao, M.; Zhang, W.; Wen, B. Dynamical modeling and multi-pulse chaotic dynamics of cantilevered pipe conveying pulsating fluid in parametric resonance. *Aero. Sci. Technol.* **2017**, *68*, 441–453. [CrossRef]

11. Bi, H.; Qi, G.; Hu, J. Modeling and analysis of chaos and bifurcations for the attitude system of a Quadrotor Unmanned Aerial Vehicle. *Complexity* **2019**, *2019*, 6313925. [CrossRef]

12. Yingjuan, Y.; Guoyuan, Q. Comparing mechanical analysis with generalized-competitive-mode analysis for the plasma chaotic system. *Phy. Lett. A* **2019**, *383*, 318–327. [CrossRef]

13. Rashid, S.; Kalsoom, H.; Hammouch, Z.; Ashraf, R.; Baleanu, D.; Chu, Y.M. New multi-parametrized estimates having pth-order differentiability in fractional calculus for predominating h-convex functions in hilbert space. *Symmetry* **2020**, *12*, 222. [CrossRef]

14. Kalsoom, H.; Vivas-Cortez, M.; Amer Latif, M.; Ahmad, H. Weighted midpoint Hermite-Hadamard-Fejer type inequalities in fractional calculus for harmonically convex functions. *Fractal Fract.* **2021**, *5*, 252. [CrossRef]

15. Ates, A. Enhanced equilibrium optimization method with fractional order chaotic and application engineering. *Neural Comput. Appl.* **2021**, *33*, 9849–9876. [CrossRef]

16. Fiaz, M.; Aqeel, M.; Marwan, M.; Sabir, M. Integer and fractional order analysis of a 3D system and generalization of synchronization for a class of chaotic systems. *Chaos Solitons Fractals* **2022**, *155*, 111743. [CrossRef]

17. Macias-Diaz, J.E. Fractional calculus & Mdash; Theory and Applications. *Axioms* **2022**, *11*, 43. [CrossRef]

18. Cafagna, D.; Grassi, G. Bifurcation and chaos in the fractional order Chen system via a time domain approach. *Int. J. Bif. Chaos* **2008**, *18*, 1845–1863. [CrossRef]

19. Liu, X.; Tang, D. Bifurcation and synchronization of a new fractional-order system. *Int. J. Dyn. Cont.* **2021**. [CrossRef]

20. Kumar, V.; Kumari, N. Stability and bifurcation analysis of fractional-order delayed prey–predator system and the effect of diffusion. *Int. J. Bif. Chaos* **2022**, *32*, 2250002. [CrossRef]

21. Bhalekar, S.; Daftardar-Gejji, V. Synchronization of different fractional order chaotic systems using active control. *Commun. Nonlin. Sci. Numer. Simul.* **2010**, *15*, 3536–3546. [CrossRef]

22. Hu, W.; Ding, D.; Zhang, Y.; Wang, N.; Liang, D. Hopf bifurcation and chaos in a fractional order delayed memristor-based chaotic circuit system. *Optik* **2017**, *130*, 189–200. [CrossRef]

23. Ndolane, S. Qualitative analysis of class of fractional-order chaotic system via bifurcation and Lyapunov exponents notions. *J. Math.* **2021**, *2021*, 5548569. [CrossRef]

24. Rajeev, K.; Sanjeev, K.; Sukhneet, K.; Shrishty, J. Time fractional generalized Korteweg-de Vries equation: Explicit series solutions and exact solutions. *J. Fract. Calculus Nonlin. Sys.* **2021**, *1*, 62–77. [CrossRef]

25. Eman, Z. Numerical solution for multi-term fractional delay differential equations. *J. Fract. Calculus Nonlin. Sys.* **2021**, *2*, 1–12. [CrossRef]

26. Qasem, M.A.M.; Mohamed, A.H.; Thabet, A. On the iterative methods for solving fractional initial value problems: New perspective. *J. Fract. Calculus Nonlin. Sys.* **2021**, *1*, 76–81. [CrossRef]

27. Safiyeh, M.; Yaghoub, M.; Farhad, D.S. Numerical solution of fractional multi-delay differential equations. *Int. J. Appl. Comput. Math.* **2022**, *8*, 1–12. [CrossRef]

28. Avcı, İ.; Mahmudov, N.I. Numerical solutions for multi-term fractional order differential equations with fractional taylor operational matrix of fractional integration. *Mathematics* **2020**, *8*, 96. [CrossRef]

29. Volos, C.K.; Pham, V.T.; Vaidyanathan, S.; Kyprianidis, I.M.; Stouboulos, I.N. Synchronization phenomena in coupled Colpitts circuits. *J. Eng. Sci. Technol. Rev.* **2015**, *8*, 142–151. [CrossRef]

30. Mofid, O.; Mobayen, S.; Khooban, M.H. Sliding mode disturbance observer control based on adaptive synchronization in a class of fractional-order chaotic systems. *Int. J. Adap. Cont. Signal Proc.* **2019**, *33*, 462–474. [CrossRef]

31. Jiang, W.; Wang, H.; Lu, J.; Cai, G.; Qin, W. Synchronization for chaotic systems via mixed-objective dynamic output feedback robust model predictive control. *J. Frank. Inst.* **2017**, *354*, 4838–4860. [CrossRef]

32. Açıkmeşe, B.; Corless, M. Observers for systems with nonlinearities satisfying incremental quadratic constraints. *Automatica* **2011**, *47*, 1339–1348. [CrossRef]

33. Zhang, W.; Su, H.; Zhu, F.; Bhattacharyya, S.P. Improved exponential observer design for one-sided Lipschitz nonlinear systems. *Int. J. Robust Nonlin. Cont.* **2016**, *26*, 3958–3973. [CrossRef]

34. Zhao, Y.; Zhang, W.; Zhang, W.; Song, F. Exponential reduced-order observers for nonlinear systems satisfying incremental quadratic constraints. *Circuits Syst. Signal Proc.* **2018**, *37*, 3725–3738. [CrossRef]

35. Gupta, M.K.; Tomar, N.K.; Darouach, M. Unknown inputs observer design for descriptor systems with monotone nonlinearities. *Int. J. Robust Nonlin. Cont.* **2018**, *28*, 5481–5494. [CrossRef]

36. Zhao, Y.; Zhang, W.; Su, H.; Yang, J. Observer-based synchronization of chaotic systems satisfying incremental quadratic constraints and its application in secure communication. *IEEE Trans. Sys. Man Cyber.* **2018**, *50*, 5221–5232. [CrossRef]

37. Sabir, M.; Marwan, M.; Ahmad, S.; Fiaz, M.; Khan, F. Observer and descriptor satisfying incremental quadratic constraint for class of chaotic systems and its applications in a quadrotor chaotic system. *Chaos Solitons Fractals* **2020**, *137*, 109874. [CrossRef]

38. Liu, L.; Shang, Y.; Di, Y.; Fu, Z.; Cai, X. Impulsive functional observer design for fractional-order nonlinear systems satisfying incremental quadratic constraints. *Circuits Syst. Signal Proc.* **2022**, *2022*, 2022. [CrossRef]

39. Boyd, S.; El Ghaoui, L.; Feron, E.; Balakrishnan, V. *Linear Matrix Inequalities in System and Control Theory*; Siam, USA, 1994; Volume 15.

40. Horn, R.A.; Johnson, C.R. *Matrix Analysis*; Cambridge University Press: Cambridge, UK, 2012.

41. Arcak, M.; Kokotovic, P. Nonlinear observers: A circle criterion design and robustness analysis. *Automatica* **2001**, *37*, 1923–1930. [CrossRef]

42. Diethelm, K. Smoothness properties of solutions of Caputo-type fractional differential equations. *Fract. Calculus Appl. Anal.* **2007**, *10*, 151–160.

43. Li, C.; Song, Y.; Wang, F.; Wang, Z.; Li, Y. A bounded strategy of the mobile robot coverage path planning based on Lorenz chaotic system. *Int. J. Adv. Rob. Syst.* **2016**, *13*, 107. [CrossRef]

44. Khan, A.; Kumar, S. Study of chaos in chaotic satellite systems. *Pramana* **2018**, *90*, 13. [CrossRef]

45. Abtahi, S.M. Melnikov-based analysis for chaotic dynamics of spin–orbit motion of a gyrostat satellite. *Proceed. Inst. Mech. Eng. Part K J. Multi-Body Dyn.* **2019**, *233*, 931–941. [CrossRef]

46. Rabha, W.I. Stability and stabilizing of fractional complex Lorenz systems. *Abst. Appl. Anal.* **2013**, *2013*, 13. [CrossRef]

47. Guoyuan, Q.; Xiaogang, Y. Modeling of a chaotic Gyrostat system and mechanism analysis of dynamics using force and energy. *Complexity* **2019**, *2019*, 13. [CrossRef]

48. Lan, Y.H.; Lan, Y.H.; Ding, L.; Zhou, Y. Full-order and reduced-order observer design for a Class of fractional-order nonlinear systems. *Asian J. Cont.* **2016**, *18*, 1467–1477. [CrossRef]

49. Ali, Z.; Muhammad, R.; Muhammad, A. Observer design for one-sided Lipschitz descriptor systems. *Appl. Math. Model.* **2016**, *40*, 2301–2311. [CrossRef]

50. Assaad, J.; Omar, N.; Abdellatif, B.M.; Nabil, D.; Mohamed, A.H. On observer design for nonlinear caputo fractional-order systems. *Asian J. Cont.* **2018**, *20*, 1533–1540. [CrossRef]

51. Younan, Z.; Wei, Z.; Wei, G.; Su, Y.; Fang, S. Exponential state observers for nonlinear systems with incremental quadratic constraints and output nonlinearities. *J. Cont. Automat. Elec. Sys.* **2018**, *29*, 127–135. [CrossRef]

52. Lazaros, M.; Mahendra, K.G.; Vikas, M.; Marwan, M.; Christos, V. Observer design for rectangular descriptor systems with incremental quadratic constraints and nonlinear outputs—Application to secure communications. *Int. J. Robust Nonlin. Cont.* **2020**, *30*, 8139–8158. [CrossRef]

53. Lazaros, M.; Aggelos, G.; Mahendra, K.G.; Christos, V.; Vikas, K.M.; Viet, T.P. Observers for rectangular descriptor systems with output nonlinearities: Application to secure communications and micro-controller implementation. *Int. J. Dyn. Cont.* **2020**, *9*, 530–540. [CrossRef]